

¹ SPARC: An Automated Workflow Toolkit for ² Accelerated Active Learning of Reactive Machine ³ Learning Interatomic Potentials

⁴ **Rahul Verma**  ¹, **Nisarg Joshi**  ¹, and **Jim Pfaendtner**  ¹

⁵ 1 Department of Chemical and Biomolecular Engineering, North Carolina State University, Raleigh, USA

DOI: [10.xxxxxx/draft](https://doi.org/10.xxxxxx/draft)

Software

- [▪ Review](#) 
- [▪ Repository](#) 
- [▪ Archive](#) 

Editor: [Evan Spotte-Smith](#)  ¹⁰

Reviewers:

- [▪ @mitwood](#)
- [▪ @anjohan](#)
- [▪ @PythonFZ](#)

Submitted: 21 September 2025 ¹⁶

Published: unpublished ¹⁷

License

Authors of papers retain copyright and release the work under a Creative Commons Attribution 4.0 International License ([CC BY 4.0](#))³⁰.

⁶ Summary

⁷ Machine learning interatomic potentials (MLIPs) are rapidly becoming an essential modeling tool, as they allow atomistic simulations to achieve larger systems and longer time scales, while retaining the accuracy of ab-initio methods. However, constructing a reactive and transferable MLIP is still challenging, as it requires high quality training data including rare events, high energy intermediates and transition states.

¹² Herein, we present SPARC (Smart Potential with Atomistic Rare events and Continuous learning), a modular Python workflow which automates the construction of reactive MLIPs that can generate chemically accurate potential energy surfaces (PES) for rare events. The idea for SPARC is to use an active learning (AL) protocol coupled with advanced sampling techniques that systematically identify new configurations and train ML models on-the-fly. The workflow consists of three main steps, which are executed iteratively in a loop until a reactive and stable MLIP is constructed. SPARC also includes utilities for visualizing configurations and plotting various properties to monitor the workflow across iterations.

¹⁸ Statement of need

²¹ While the AL protocol ([Podryabinkin & Shapeev, 2017](#)) ([Mikscha et al., 2021](#)) has become a standard approach to refine ML models, it does not guarantee access to kinetically or thermodynamically rare events. Many learning schemes for MLIP invoke the use of higher temperature simulations to enhance phase space exploration. Even so, without additional enhanced sampling there is little to no possibility of systematically achieving reliable reactive MLIPs.

²⁷ The motivation behind SPARC is to simplify the generation of high-quality training data and minimize the level of manual intervention required from the user. Although AL strategies have already proven effective for expanding training datasets, their integration with enhanced sampling techniques have typically been done in an ad hoc and largely manual manner. This makes it difficult to generalize these workflows beyond the original problem and limits reproducibility.

³³ Several groups have coupled AL with enhanced sampling or pathway exploration techniques. Vitartas et al. ([Vitartas et al., 2025](#)) combined AL with well-tempered metadynamics to study organic reactions in both gas phase and solvent. Rivero et al. ([Rivero et al., 2019](#)) trained PhysNet architecture together with an AL at 1000K MD for Diels–Alder and hydrogen transfer reactions. Ang et al. ([Ang et al., 2021](#)) used SchNet combined with nudged elastic band calculations to explore solvent effects on pericyclic reactions. Parrinello and coworkers ([Niu et al., 2020](#)) coupled AL with variational enhanced sampling using DeePMD to investigate the

40 phase diagram of gallium. Zhao et al. (Zhao et al., 2022) introduced a workflow combining
 41 umbrella sampling with AL to map out the solid-phase transition of GeSbTe. These studies
 42 highlight the promise of AL combined with enhanced sampling, but they remain highly tailored
 43 and driven by use case-specific implementations that can be difficult to generalize or reproduce.
 44 SPARC automates this process by integrating the PLUMED library (Tribello et al., 2014) with
 45 AL protocol into a single modular workflow (see Figure 1). This allows user to use any advance
 46 sampling technique implemented in PLUMED to explore the configurational space and finding
 47 reactive configurations enabling scalable and reproducible MLIPs for generalized chemical
 48 environment.

49 Features and Implementation

50 SPARC is written in Python and can run on both local workstations and high-performance
 51 clusters. We utilized the Atomic Simulation Environment (ASE) (Larsen et al., 2017) library
 52 as the brain for SPARC which enables seamless integration of the MD engine, machine learning
 53 architecture, and electronic structure codes. To ensure portability, SPARC implements a file-
 54 based management system, and the output of each stage is written in a structured directory. The
 55 workflow iterations are stored in subdirectories (iter_000000, iter_000001,), with subfolders
 56 for reference first principle (FP) calculations (00.dft), MLIP training (01.train), and ML/MD
 57 simulations (02.dpmd). The SPARC workflow is controlled through a single YAML configuration
 58 file.
 59 SPARC currently supports VASP (Hafner, 2008) and CP2K (Hutter et al., 2014) for electronic
 60 structure calculation, although this could be readily expanded in the future. For MLIP training
 61 we use DeePMD-kit architecture (Wang et al., 2018), with the ensemble model approach for
 62 query-by-committee (QbC) uncertainty estimation (Mikschat et al., 2021). ML/MD simulations
 63 are run using ASE MD engine coupled together with both DeePMD and PLUMED calculator.
 64 ML/MD output is stored in ASE trajectory formats as this enables the broader ecosystem of
 65 analysis tools that already support ASE compatible formats. Since SPARC manages all stages
 66 via ASE, the workflow requires a Python environment with necessary dependencies. This makes
 67 the workflow highly portable across computing environments and suitable for both exploratory
 68 studies and large-scale production run.

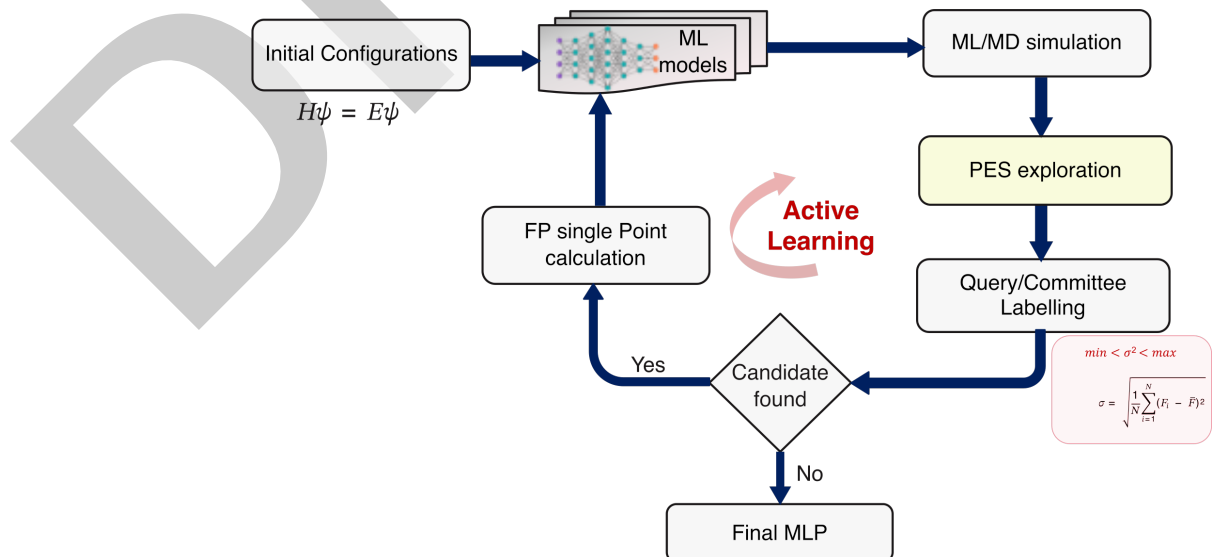


Figure 1: A schematic representation of AL cycle for training MLIPs. SPARC implements an additional block (PES exploration) to this cycle for systematic exploration of the configurational space.

69 Technical requirements and usage examples

70 After installation, a typical SPARC workflow can be launched with a single command:

```
sparc -i input.yaml
```

71 Illustrative Example: Potential Energy Scan

72 To illustrate the capabilities of SPARC, we applied the workflow to a simple ammonia borate
 73 (NH_3BH_3) molecule. The goal is to demonstrate how SPARC systematically expands training
 74 data and improves the accuracy of MLIPs through iterative learning. The initial training
 75 dataset only has 64 configurations, generated by scanning the B-N bond at the semiempirical
 76 level, followed by DFT single point calculations at PBE level with energy cutoff of 300 eV
 77 in VASP.

78 An ensemble of DeePMD models were trained and one of the ML models was used to run MD
 79 simulation for 5 ns with a timestep of 1 fs for each iteration. To ensure exploration beyond
 80 equilibrium structures, enhanced sampling was employed using parallel bias metadynamics
 81 (PbMetaD) (Pfaendtner & Bonomi, 2015) on SPRINT collective variables (Pietrucci &
 82 Andreoni, 2011). We obtain the uncertainty in forces by using an ensemble of trained models
 83 within QbC approach (Mikscha et al., 2021) to flag configurations. Then configurations with
 84 standard deviation in the atomic forces between 0.05 to 0.5 eV/Å were automatically flagged
 85 and labeled with DFT. These structures were then added into the existing training dataset,
 86 after which the DeePMD models were retrained to get updated potential for the next cycle.

87 The effect of this iterative refinement is shown in Figure 2 which plots the maximum force
 88 deviation recorded in each cycle. In the initial iterations, deviations were large. As the workflow
 89 explores the chemical space and finds new configurations, these errors slowly decreased,
 90 indicating that the model was progressively learning the relevant physics.

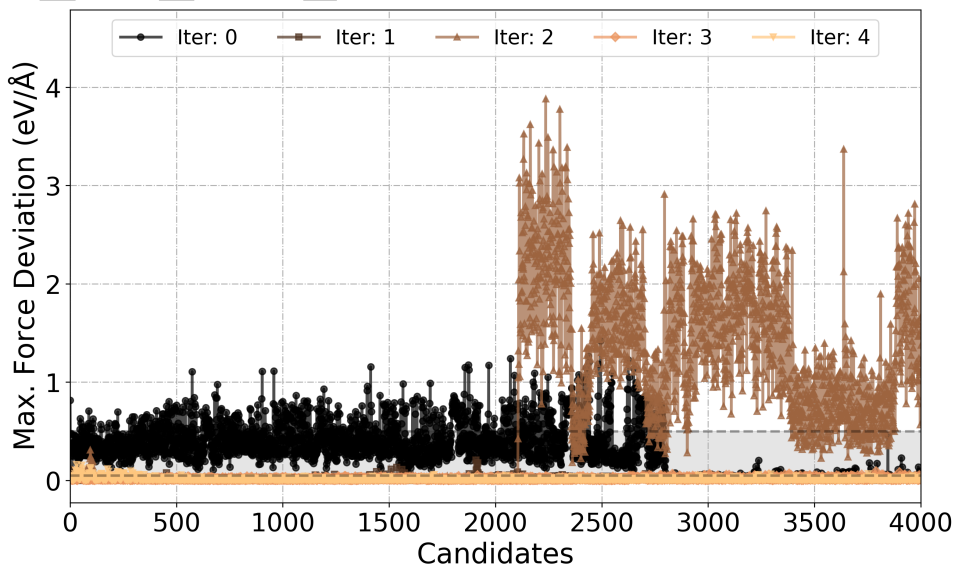


Figure 2: Force deviation across SPARC iterations. The shaded region marks the uncertainty thresholds for labeling.

91 By the fourth iteration, the error had converged to near-zero values, reflecting a stable and
 92 reactive MLIP. During exploration the model will be exposed to new configurations beyond
 93 training data which can result in very high forces, as observed in iteration 2.

⁹⁴ We further assessed the reliability of trained MLIP under finite-temperature molecular dynamics.
⁹⁵ We performed enhanced sampling MD for both ab-initio and ML. In these simulations, the
⁹⁶ B-N bond distance was biased with metadynamics with a Gaussian width 0.05 Å and height
⁹⁷ 0.005 eV. The resulting free energy profile is shown in [Figure 3](#).

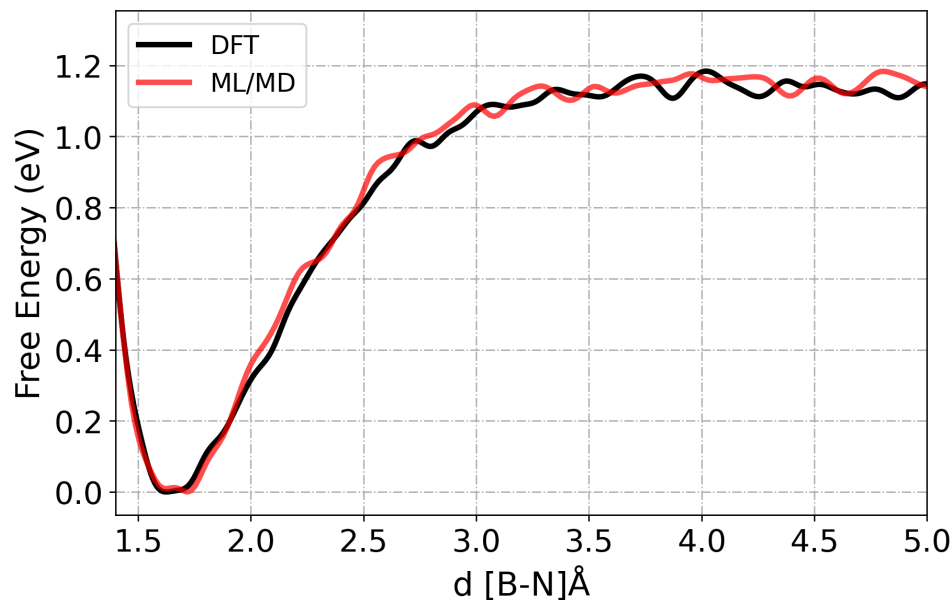


Figure 3: Free energy profile computed from both AIMD (black) and MLIP (red).

⁹⁸ Here, MLIP was able to reproduce minima near 1.6 Å, with some minor discrepancies after 3.0
⁹⁹ Å. The root mean square deviation between these curves was 0.04 eV, which is within chemical
¹⁰⁰ accuracy.

¹⁰¹ These results demonstrate MLIP trained with our workflow not only reproduces potential
¹⁰² energy surface but also able to estimate quantitatively reliable predictions for computing free
¹⁰³ barriers and investigating chemical reactions.

104 Acknowledgements

¹⁰⁵ This work was partially supported by NSF award EFRI-2132219 to RV and JP, and the HPC
¹⁰⁶ facility at the NC State University.

107 Related software

¹⁰⁸ SPARC interface builds upon the following packages:

- ¹⁰⁹ **ASE**: atomic simulation setup, DFT calculators, and file handling.
- ¹¹⁰
- ¹¹¹ **DeePMD-kit**: MLIP training and deployment.
- ¹¹²
- ¹¹³ **PLUMED**: enhanced sampling and CV biasing.
- ¹¹⁴
- ¹¹⁵ **VASP** and **CP2K**: first-principles labeling.

116 References

- 117 Ang, S. J., Wang, W., Schwalbe-Koda, D., Axelrod, S., & Gómez-Bombarelli, R. (2021).
118 Active learning accelerates ab initio molecular dynamics on reactive energy surfaces. *Chem*,
119 7(3), 738–751. <https://doi.org/10.1016/j.chempr.2020.12.009>
- 120 Hafner, J. (2008). Ab-initio simulations of materials using VASP: Density-functional theory
121 and beyond. *Journal of Computational Chemistry*, 29(13), 2044–2078. <https://doi.org/10.1002/jcc.21057>
- 123 Hutter, J., Iannuzzi, M., Schiffmann, F., & VandeVondele, J. (2014). CP2K: Atomistic
124 simulations of condensed matter systems. *Wiley Interdisciplinary Reviews: Computational
125 Molecular Science*, 4(1), 15–25. <https://doi.org/10.1002/wcms.1159>
- 126 Larsen, A. H., Mortensen, J. J., Blomqvist, J., Castelli, I. E., Christensen, R., Dułak, M., Friis,
127 J., Groves, M. N., Hammer, B., Hargus, C., & others. (2017). The atomic simulation
128 environment—a python library for working with atoms. *Journal of Physics: Condensed
129 Matter*, 29(27), 273002. <https://doi.org/10.1088/1361-648X/aa680e>
- 130 Miksch, A. M., Morawietz, T., Kästner, J., Urban, A., & Artrith, N. (2021). Strategies
131 for the construction of machine-learning potentials for accurate and efficient atomic-
132 scale simulations. *Machine Learning: Science and Technology*, 2(3), 031001. <https://doi.org/10.1088/2632-2153/abfd96>
- 134 Niu, H., Bonati, L., Piaggi, P. M., & Parrinello, M. (2020). Ab initio phase diagram and
135 nucleation of gallium. *Nature Communications*, 11(1), 2654. <https://doi.org/10.1038/s41467-020-16372-9>
- 137 Pfaendtner, J., & Bonomi, M. (2015). Efficient sampling of high-dimensional free-energy
138 landscapes with parallel bias metadynamics. *Journal of Chemical Theory and Computation*,
139 11(11), 5062–5067. <https://doi.org/10.1021/acs.jctc.5b00846>
- 140 Pietrucci, F., & Andreoni, W. (2011). Graph theory meets ab initio molecular dynamics:
141 Atomic structures<? Format?> And transformations at the nanoscale. *Physical Review
142 Letters*, 107(8), 085504. <https://doi.org/10.1103/PhysRevLett.107.085504>
- 143 Podryabinkin, E. V., & Shapeev, A. V. (2017). Active learning of linearly parametrized
144 interatomic potentials. *Computational Materials Science*, 140, 171–180. <https://doi.org/10.1016/j.commatsci.2017.08.031>
- 146 Rivero, U., Unke, O. T., Meuwly, M., & Willitsch, S. (2019). Reactive atomistic simulations
147 of diels-alder reactions: The importance of molecular rotations. *The Journal of Chemical
148 Physics*, 151(10). <https://doi.org/10.1063/1.5114981>
- 149 Tribello, G. A., Bonomi, M., Branduardi, D., Camilloni, C., & Bussi, G. (2014). PLUMED
150 2: New feathers for an old bird. *Computer Physics Communications*, 185(2), 604–613.
151 <https://doi.org/10.1016/j.cpc.2013.09.018>
- 152 Vitartas, V., Zhang, H., Juraskova, V., Johnston-Wood, T., & Duarte, F. (2025). Active
153 learning meets metadynamics: Automated workflow for reactive machine learning potentials.
154 *ChemRxiv*. <https://doi.org/10.26434/chemrxiv-2024-twmlz>
- 155 Wang, H., Zhang, L., Han, J., & E, W. (2018). DeePMD-kit: A deep learning package for
156 many-body potential energy representation and molecular dynamics. *Computer Physics
157 Communications*, 228, 178–184. <https://doi.org/10.1016/j.cpc.2018.03.016>
- 158 Zhao, Y., Sun, J., Yang, L., Zhai, D., Sun, L., & Deng, W. (2022). Umbrella sampling with
159 machine learning potentials applied for solid phase transition of GeSbTe. *Chemical Physics
160 Letters*, 803, 139813. <https://doi.org/10.1016/j.cplett.2022.139813>